

Influence of aerostatic force on measuring the aerodynamic moment during the torsional oscillation of a linear blade cascade

*Volodymyr Tsymbalyuk and Petr Eret**

University of West Bohemia, Faculty of Mechanical Engineering, Department of Power System Engineering, Univerzitní 22, Pilsen 30614, Czech Republic

Abstract. An improved method of measuring unsteady aerodynamic moments at torsional oscillations of flexibly mounted blades in a linear cascade is presented. Specifically, a systematic error was found in measuring the real part of the unsteady aerodynamic moment (not affecting system stability). The error cause is identified as a change in the torsional stiffness of the elastic suspension of the blade profile under the influence of a stationary aerodynamic force. A mathematical model for error compensation is developed and successfully applied, improving the measurement method.

1 Introduction

Flutter in turbomachinery is a phenomenon of self-excited blade vibrations. It is caused by unsteady aerodynamic forces and moments that arise due to the interaction between the blade vibrations and a fluid flow. Aeroelastic instability occurs when a specific mode of blade row vibration absorbs energy from the fluid flow. Flutter leads to the accumulation of fatigue damage when a blade is subjected to low-amplitude oscillations over a prolonged period. When the vibration amplitude becomes too large, flutter results in rapid blade damage and poses a threat to the safety of turbomachinery.

Experimental studies of turbomachinery blade flutter are important for understanding this phenomenon and validating CFD models [1-4]. So far, most cascade data have been obtained using experiments on two-dimensional subsonic and transonic flows with oscillating turbine and compressor cascade blades. Many authors have reported that the mode shape is the most significant factor in determining blade cascade aerodynamic stability.

At the Department of Power System Engineering, University of West Bohemia, a wind tunnel with a methodology for measuring unsteady aerodynamic forces and moments in a vibrating linear blade cascade was developed [5, 6]. Like any other highly specialized method, the testing has limitations and measurement errors. Therefore, it is important to identify and compensate for systematic measurement errors. For example, when measuring aerodynamic forces and moments acting on flexibly mounted non-rigid blade profiles, the

* Corresponding author: petreret@fst.zcu.cz

effect of blade profile deformation must be accounted for to improve the accuracy of determining the aerodynamic work per the oscillation cycle and the flutter boundary [7, 8].

The experimental and CFD investigation of aerodynamic forces and moments in a linear turbine blade cascade in [9] showed that the imaginary part of the unsteady fluid coefficient, proportional to the aerodynamic work and thus to system stability, is in reasonable agreement with both approaches. In contrast, the experimentally obtained real part of the unsteady fluid coefficient for the aerodynamic moment differed from the simulated data. Therefore, this paper presents further investigation to reveal the cause of the discrepancy in the results.

2 Measurement method

The method of measuring unsteady aerodynamic forces and moments in a vibrating linear blade cascade and the experimental setup are detailed in [5, 6], and only the basic principles are mentioned here. A subsonic wind tunnel with a cascade of eight blades in total and four flexibly mounted blades in the middle is employed. The tested blade profile represents a reduced section of the tip profile of the last-stage blade of the steam turbine rotor. Figure 1 shows a flexible blade suspension with two degrees of freedom. Two elastic elements of different widths enable bending and torsion motions, forming an elastic parallelogram that ensures limited tilting of the blade profile.

Since the directions of the measured unsteady aerodynamic force and moment coincide with the directions of the motions y and α , electrodynamic vibrators can be used to excite vibrations and to measure the loads. According to the Ampere law, the force induced by the vibrator can be determined from the magnitude of the current i_c as in Eq.1,

$$F = Bl_c i_c, \quad (1)$$

where l_c is the length of the coil and B is the magnetic field induction.

The bending and torsion motion of the n^{th} blade ($n = 3$ to 6) is described by Eq. 2,

$$y_n = Y \sin[\omega t + (n-3) \cdot IBPA], \quad \alpha_n = A \sin[\omega t + (n-3) \cdot IBPA + \eta] \quad (2)$$

where Y is the bending amplitude, A is the torsion amplitude, ω is the angular frequency at the excitation, IBPA means the inter blade phase angle (0 to 360 deg with a step of 30 deg), η is the phase angle between bending and torsional movements, t is the time.

The force and moment equations for the pair of vibrators can be written in Eq. 3,

$$F_v = F_1 + F_2, \quad M_v = h(F_1 - F_2) \quad (3)$$

where F_1 and F_2 are the forces generated in coils the and h is the between-axis distance defined in Fig. 1.

When the flexibly mounted blade is subject to flow, aerodynamic force L_A and moment M_A are generated. Hence, the equation of motion of the 2dof system under the influence of fluid flow is as Eq. 4,

$$\begin{cases} m\ddot{y} + q_y\dot{y} + K_y y + mx_m\ddot{\alpha} = L_A + F_v \\ I\ddot{\alpha} + q_\alpha\dot{\alpha} + K_\alpha \alpha + mx_m\dot{y} = M_A + M_v, \end{cases} \quad (4)$$

where m is the mass of the suspension with the airfoil, I is the inertia moment about the rotation axis, x_m is the coordinate of the centre of mass; K_y , K_α are the coefficients of mechanical stiffness; q_y , q_α are the coefficients of mechanical damping in respective directions.

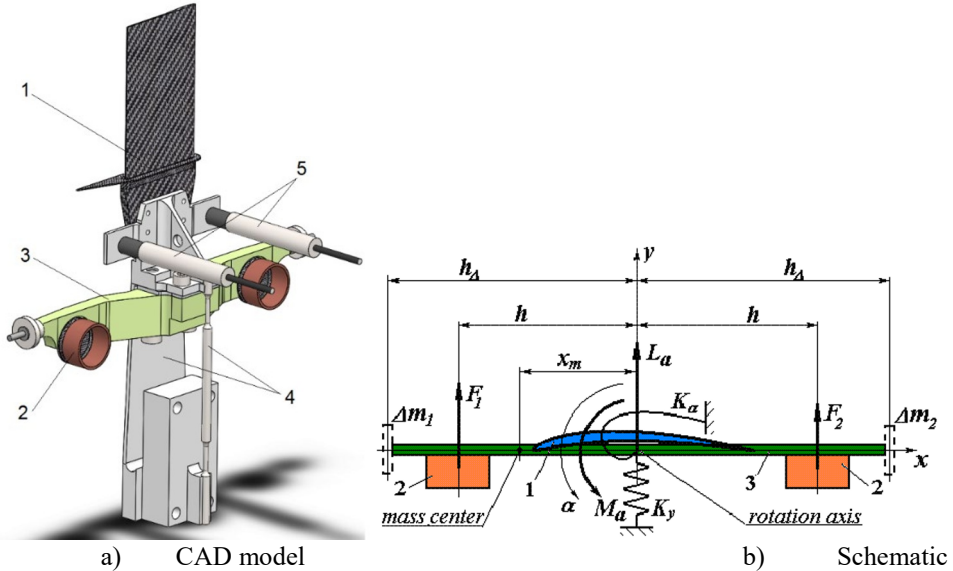


Fig.1. Blade flexible suspension, 1 - blade profile; 2 – electromagnetic shaker coil; 3 - cross-beam; 4 - elastic elements; 5 - displacement sensors; Δm_1 , Δm_2 - calibration masses (arrows indicate positive directions of aerodynamic loading and blade motions).

When the flow is absent, the aerodynamic load is zero $L_A = 0$, $M_A = 0$, and the equation of motion is as in Eq. 5,

$$\begin{cases} m\ddot{y} + q_y\dot{y} + K_y y + mx_m\ddot{\alpha} = F_{v0} \\ I\ddot{\alpha} + q_\alpha\dot{\alpha} + K_\alpha\alpha + mx_m\dot{y} = M_{v0}, \end{cases} \quad (5)$$

where F_{v0} and M_{v0} are the force and moment of the pair of vibrators in the case of vibration with no flow. Moreover, if the amplitude vibration of the suspension is maintained constant with and without flow, then after subtracting Eq. 5 from Eq.4, the equations' left-hand sides are cancelled out and aerodynamic loads can be defined as in Eq. 6.

$$L_A = F_{v0} - F_v, \quad M_A = M_{v0} - M_v \quad (6)$$

The unsteady aerodynamic force L_A and the aerodynamic moment M_A are complex; only the imaginary parts contribute to the system's stability. In this work, the real parts of the aerodynamic loading as a function of IBPA are the subject of further investigation.

2 Influence of aerostatic force on the aerodynamic moment

In addition to the previously obtained results [9], Fig. 2 depicts the comparison between the measured (M) and simulated data (CFD) of the real part of the unsteady aerodynamic moment coefficient at the torsional oscillation for each flexibly mounted blade (#3-6). A systematic data shift between the results of both techniques tested is evident in all plots. The experimental datasets for blades #3 and #4 yield higher values of the real part of the unsteady aerodynamic moment coefficient, while blades #5 and #6 show the opposite. These results were achieved for inlet isentropic Mach number = 0.34 and angle of incidence = $+5^\circ$ with the torsion vibration amplitude = 0.5° .

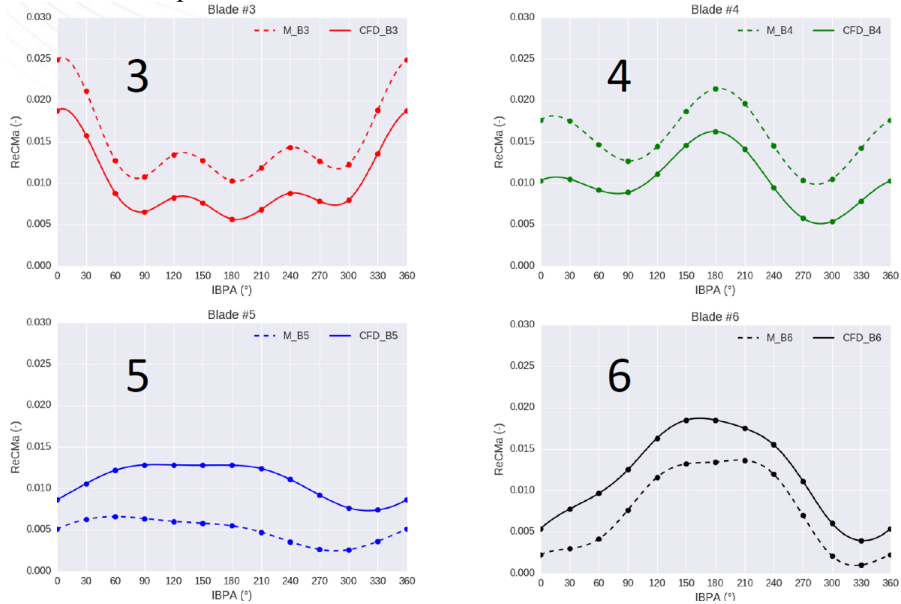


Fig.2 Comparison between the measured (M) and simulated data (CFD) of the real part of the unsteady aerodynamic moment coefficient at the torsional oscillation for each flexibly mounted blade (#3-6).

Inspection of the placement of the vibration units on a supporting frame (see Fig. 3) can provide a possible explanation for the data shift.

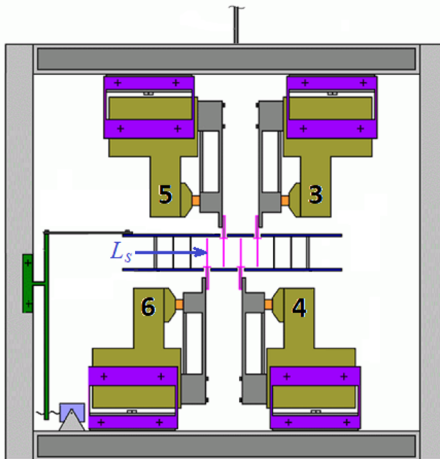


Fig.3. Blade cascade flexible suspensions on a supporting frame, upstream view.

The aerostatic force L_s compresses the flexible suspensions of blades #3 and #4 towards the rigid parts of electromagnetic shakers, while the effect of this force on blades #5 and #6 is the opposite. This finding allows us to assume that the aerostatic force L_s may affect the torsional stiffness of the elastic suspension by generating an additional moment.

Fig. 4a shows the bending moment distribution along the wide elastic element caused by the static load L_s . In a cross-section at half the length of the elastic parallelogram, the bending moment of a wide part of the elastic element of rectangular shape is zero. The force P_l acting along the narrow elastic element can be expressed by Eq. 7,

$$P_l = L_s \cdot \frac{l}{H} \quad (7)$$

where l is the distance between the point of application of force L_s and the zero bending moment point, and H is the distance between the elastic parts of the parallelogram, as shown in Fig. 4.

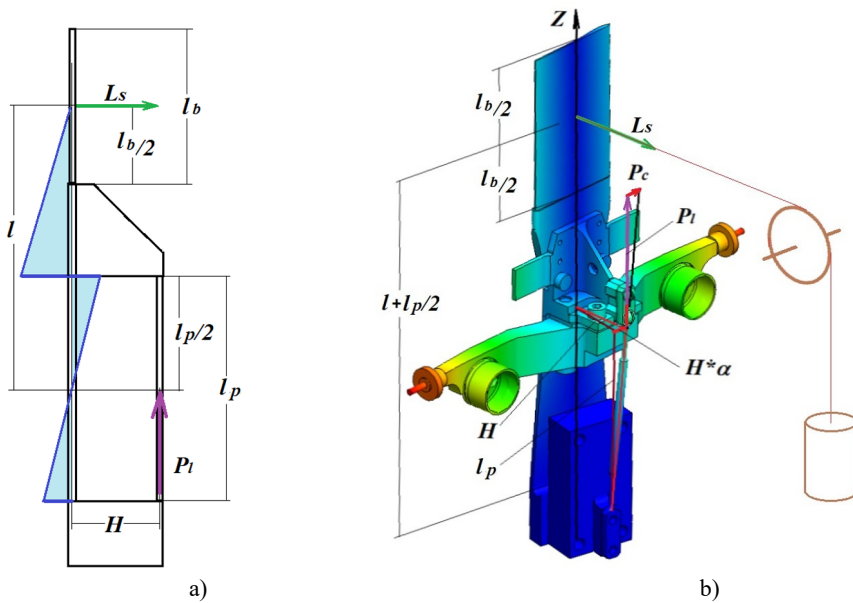


Fig.4. Blade flexible suspension with a static load model.

During the torsion motion with an angle α about the Z -axis, the narrow elastic element tilts to the side with a distance of $H \cdot \alpha$ (see Fig. 4b), and the force P_l creates a transverse force P_c given by Eq. 8.

$$P_c = P_l \cdot \frac{H \cdot \alpha}{l_p} = L_s \cdot \frac{l}{l_p} \cdot \alpha \quad (8)$$

Additional torsion moment about the Z -axis can be expressed using Eq. 9,

$$M_c = P_c \cdot H = L_s \cdot K_p \cdot \alpha \quad (9)$$

where $K_p = \frac{l}{l_p} \cdot H$.

A simple pulley experiment with a known weight was performed to estimate the additional moment M_{ex} for torsion motion under the influence of a static loading acting in the middle of the blade height, as shown in Fig. 4b. This testing was carried out for both directions of the static load action for the torsion motion amplitude $\alpha_{ex} = 0,5$ deg (0,00873 rad). Fig. 5 details the experimental results showing the dependence of the additional moment on the static force. The imaginary part of the additional moment practically does not depend on the static force, while the real part is linearly dependent. In addition, the parameter K_p in Eq. 9 can also be experimentally evaluated by Eq. 10, leading to good agreement between the two values (error 2.5% only).

$$K_{p_{ex}} = \frac{M_{c_{ex}}}{L_s \cdot \alpha_{ex}} = 0.05443 [m] \quad (10)$$

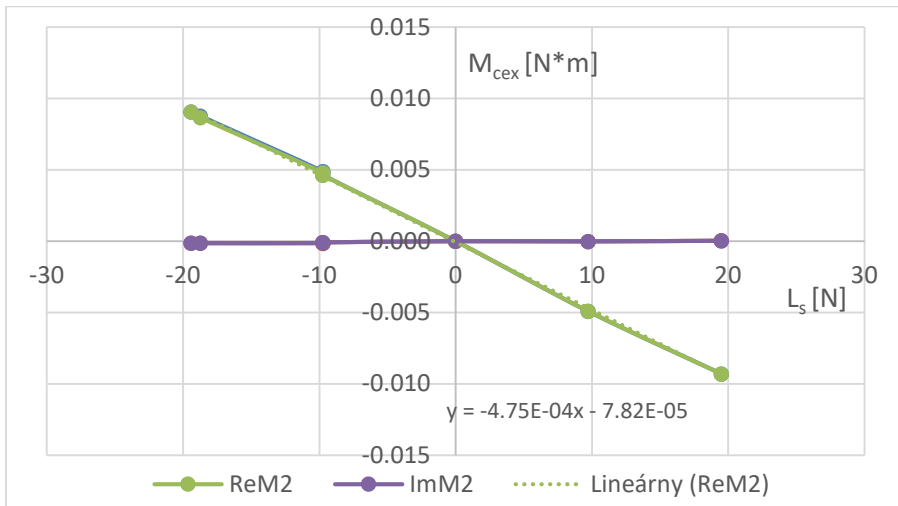


Fig.5. A dependence of the additional moment on a static force during torsional oscillation.

As a result of the above finding, the blade flexible suspension in a fluid flow under the influence of aerostatic force will have a different torsional stiffness than without flow. Hence Eq. 3 can be modified as Eq. 11.

$$\begin{cases} m\ddot{y} + q_y \dot{y} + K_y y + mx_m \ddot{\alpha} = L_A + F_v \\ I\ddot{\alpha} + q_\alpha \dot{\alpha} + K_\alpha \alpha - L_s \cdot K_p \cdot \alpha + mx_m \dot{y} = M_A + M_v \end{cases} \quad (11)$$

After subtracting Eq. 4 from Eq. 11, the corrected unsteady aerodynamic forces and moments are obtained in Eq. 12.

$$L_A = F_{v0} - F_v, \quad M_A = M_{v0} - M_v - L_s \cdot K_p \cdot \alpha. \quad (12)$$

Finally, the parameter K_p is negative for blades #3 and #4 and positive for blades #5 and #6.

3 Results including the influence of aerostatic force

Fig. 6 shows the real part of the unsteady aerodynamic moment for blade #4 using simulated, original and corrected experimental data. Including the correction parameter K_p yields excellent agreement between the experimental data and the CFD results. Similar improved results are obtained for other blades (not shown here).

The real part of the unsteady aerodynamic moment affects the oscillation frequency of the blades in the flow, but this effect is minimal for turbine blades. Therefore, the proposed correction does not fundamentally affect the measurement results but is important for numerical data validation.

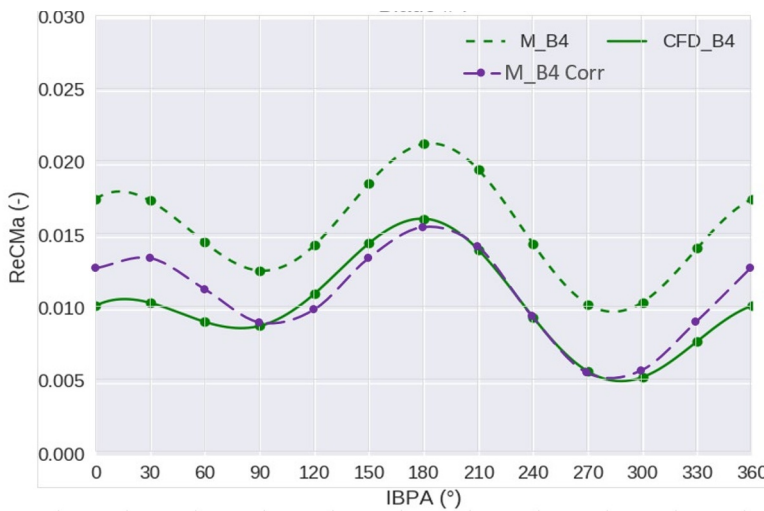


Fig.6. The real part of the unsteady aerodynamic moment for the blade #4 using simulated (CFD), original (M) and corrected (M Corr) experimental data.

Conclusions

The paper presents an improved method of measuring the unsteady aerodynamic moment during the torsional oscillation of a linear blade cascade. In detail, a systematic error was found in measuring the real part of the aerodynamic moment. By inspecting the previously obtained results and the placement of the vibration units on a supporting frame, an assumption of an aerostatic force affecting the torsional stiffness of the elastic suspension by generating an additional torsion moment was proposed. A detailed model based on the bending moment distribution along the wide elastic element caused by the static load was developed, and the additional torsion moment was formulated. Moreover, an auxiliary experiment was performed, and a correction parameter related to the additional torsion moment was evaluated and implemented into the methodology. Finally, the real part of the unsteady aerodynamic moment for blade #4 was shown using simulated, original and corrected experimental data. Including the correction parameter yielded excellent agreement between the experimental data and the CFD results.

Acknowledgements

This project is co-financed with the state support of the Technology Agency of the Czech Republic as part of the Program for the Support of Applied Research, Experimental Development and Innovation of the National Center of Competence (TN02000025).

References

1. H. Ma, C. Jin, W. Wei, Experimental Investigation of Effects of Suction Side Squealer Tip on the Aeroelastic Stability of a Linear Oscillating Compressor Cascade, *Proc. Inst. Mech. Eng., Part G: J. Aerosp. Eng.*, **231(11)**, pp. 2120–2131 (2017).
2. C. E. Seeley, C. Wakelam, X. Zhang, D. Hofer, W.-M. Ren, Investigations of Flutter and Aerodynamic Damping of a Turbine Blade: Experimental Characterization, *ASME J. Turbomach.*, **139(8)**, p. 081011 (2017)
3. L. Malzacher, S. Geist, V. Motta, D. Peitsch, H. Hennings, A Low-Speed Compressor Test Rig for Flutter Investigations, *ASME J. Turbomach.*, **141(5)**, p. 051009 (2019)
4. P. Jutur, R. N. Govardhan, Flutter in Started and Unstarted Transonic Linear Cascades: Simultaneous Measurements of Unsteady Loads and Shock Dynamics, *ASME J. Turbomach.*, **141(12)**, p. 121004 (2019)
5. V.A. Tsimbalyuk, Method of Measuring Transient Aerodynamic Forces and Moments on Vibrating Cascade, *Strength of Materials*, vol. 28, no. 2, pp. 150-157, (1996)
6. P. Eret, V. Tsimbalyuk, Experimental Subsonic Flutter of a Linear Turbine Blade Cascade With Various Mode Shapes and Chordwise Torsion Axis Locations, *Journal of Turbomachinery*, **145(6)**:1-12, (2023)
7. V. Tsimbalyuk, J. Linhart, Corrections of aerodynamic loadings measurement on vibrating airfoils, *Proceedings, XVII IMEKO Congress, Dubrovnik, Croatia*, pp. 358-361. June 22-27, (2003), ISBN 953-7124-00-2
8. S. Kabannik, V. Tsimbalyuk, Special features of the measurement of aerodynamic forces on an airfoil under flexural vibrations, *Proceeding, XV Conference "Power system engineering, thermodynamics & fluid flow, West Bohemian university in Pilsen, Czech Republic*, (2016). ISBN 978-80-261-0626-5.
9. V. Slama, B. Rudas, J. Ira, A. Macalka, P. Eret, V. Tsimbalyuk, Experimental and CFD Investigation of Aerodynamic Forces and Moments in a Linear Turbine Blade Cascade. Volume **4A**: Dynamics, Vibration, and Control. ASME International Mechanical Engineering Congress and Exposition, Proceedings (IMECE) Volume 4A-20182018 ASME 2018 International Mechanical Engineering Congress and Exposition, IMECE 2018, Pittsburgh, 9 November 2018 through 15 November (2018), Code 144113, doi:10.1115/imece2018-86667